

Unraveling the Mechanism of Cascade Reactions of Zincke Aldehydes

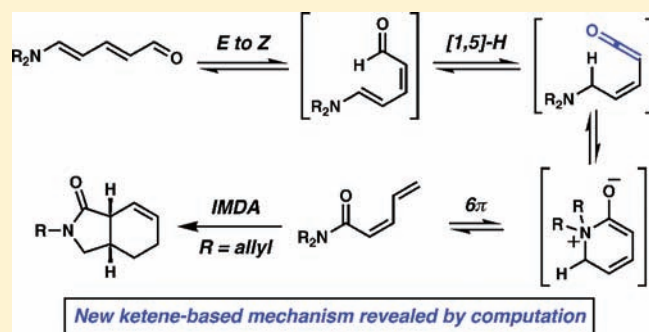
Robert S. Paton,[†] Sarah E. Steinhardt,[‡] Christopher D. Vanderwal,^{*,‡} and K. N. Houk^{*,†}

[†]Department of Chemistry and Biochemistry, University of California, Los Angeles, 607 Charles E. Young Drive, Los Angeles, California 90095-1569, United States

[‡]Department of Chemistry, University of California, Irvine, 1102 Natural Sciences II, Irvine, California 92697-2025, United States

S Supporting Information

ABSTRACT: The thermal pericyclic cascade rearrangement of Zincke aldehydes (5-(dialkylamino)-2,4-pentadienals) to afford *Z*- $\alpha,\beta,\gamma,\delta$ -unsaturated amides discovered by the Vanderwal group has been studied in depth using quantum mechanical methods. Two mechanistic possibilities that had previously been put forth to explain this internal redox process, one that had been discounted by experiment and the other that had withstood experimental scrutiny, were evaluated. Both of these mechanisms suffered from energetic barriers that appeared too high to allow rearrangement to proceed under the conditions used; however, computational study of a third possibility that implicates the intermediacy of vinylketenes revealed that it is the most likely pathway of rearrangement. Further computational studies accounted for the relative rates of rearrangement in substituted Zincke aldehydes, predicted the feasibility of related processes for other donor–acceptor dienes, and provided insight into the rearrangement of allylamine-derived Zincke aldehydes that provide either dihydropyridones or polycyclic lactams by further pericyclic processes.



INTRODUCTION

Pericyclic cascade reactions frequently provide rapid access to useful molecular architectures. The complete understanding of the mechanisms of cascade rearrangements can lead to the design of new productive tandem processes. The Vanderwal group reported the thermal pericyclic cascade rearrangement reactions of Zincke aldehydes (5-(dialkylamino)-2,4-pentadienals),¹ which are readily available from the ring-opening of pyridinium salts, in 2008 (Scheme 1).^{2,3} The products of these reactions were *Z*- $\alpha,\beta,\gamma,\delta$ -unsaturated amides, compounds that in many cases would be difficult to access in a stereocontrolled manner by other means. The following year, Zincke aldehydes derived from allylic or homoallylic amines were found to undergo this same rearrangement process followed by an efficient, stereoselective intramolecular Diels–Alder cycloaddition reaction to afford complex, polycyclic lactams.⁴ The chemistry of Zincke aldehydes has been studied extensively in the Vanderwal group,^{5–8} with recent applications including the synthesis of the core of the *Strychnos*, *Aspidosperma*, and *Iboga* alkaloids⁷ and the formal synthesis of the antitumor antibiotics porothramycins A and B.⁸

We have now evaluated the feasibility of the various possible rearrangement pathways of Zincke aldehydes with quantum mechanical calculations, employing high-level composite ab initio methods. A new mechanism is established that is predicted to be strongly favored over competing pathways. We present strong computational support for a reaction pathway involving the intermediacy of vinylketenes in the cascade rearrangement of

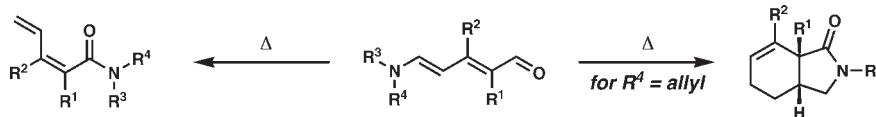
Zincke aldehydes. The trends in relative rates of rearrangement of substituted Zincke aldehydes are predicted by computation, and experiments to intercept the ketene intermediates by other means are described. Computed barriers of activation for substituted cases have been tested in experimental studies. Competing pericyclic cascade mechanisms of Zincke aldehydes derived from allylic amines were studied computationally, and the possible sigmatropic and electrocyclic pathways are discussed. The possibility of thermal rearrangements of oxygen and sulfur analogues of the original amino-2,4-pentadienal substrates are investigated computationally, and we discuss the potential of these reactions to deliver *Z*- $\alpha,\beta,\gamma,\delta$ -unsaturated esters and thioesters, respectively. We have also investigated the mechanism of a previously described rearrangement of polychlorinated 5-mercapto-2,4-pentadienals, and our results suggest that an alternative mechanism to that found for the Zincke aldehydes is preferred. The detailed understanding of these cascade reactions should enable the development of new, broadly useful rearrangement reactions to access value-added architectures.

RESULTS AND DISCUSSION

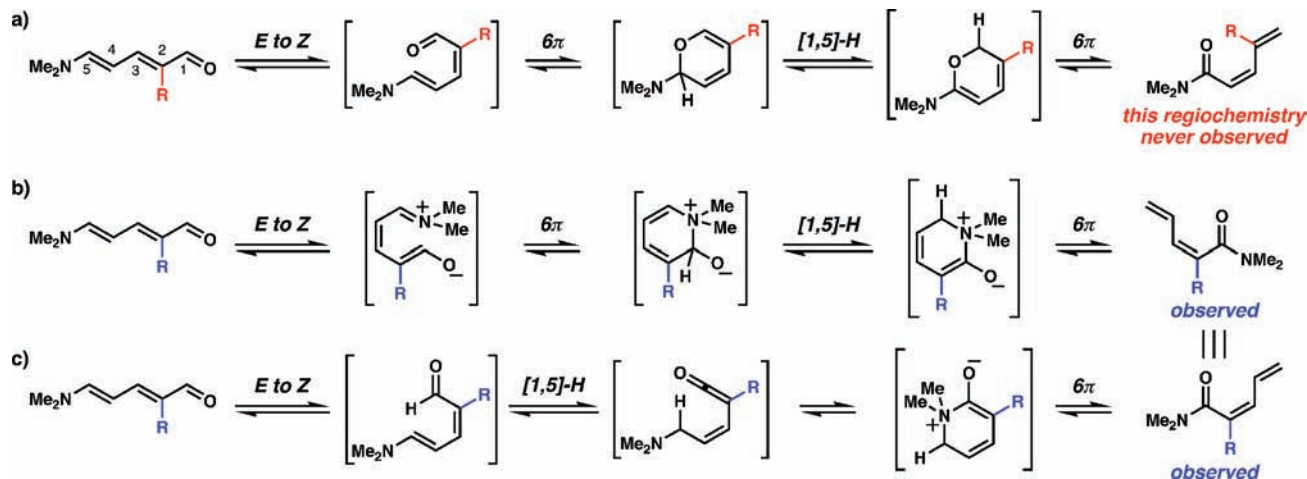
The first paper from the Vanderwal group in this area¹ described two reasonable mechanistic scenarios to account for the internal redox process that delivers the unsaturated amide

Received: September 13, 2010

Published: February 25, 2011

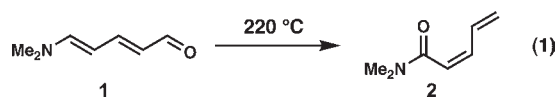
Scheme 1. Rearrangements of Zincke Aldehydes Afford Z - $\alpha,\beta,\gamma,\delta$ -Unsaturated Amides and Polycyclic Lactams

Scheme 2. Mechanistic Possibilities for the Rearrangements of Zincke Aldehydes



products from Zincke aldehydes, one that was formally the transposition of the carbonyl oxygen from one terminus of the molecule to the other and a second that required the transposition of the dialkylamino group (Scheme 2a,b). The first possibility was readily ruled out by the regiochemistry observed in the reactions of substituted Zincke aldehydes; however, the mechanism consisting of initial double bond isomerization, 6π -electrocyclic ring closure, [1,5]-sigmatropic shift of hydrogen, and 6π -electrocyclic ring-opening was considered to be sound. We have now investigated a third mechanism (Scheme 2c) involving a change in the order of events, such that the [1,5]-sigmatropic shift of hydrogen precedes ring closure. Computations show that this is the preferred pathway.

The rearrangement of 5-(dimethylamino)-2,4-pentadienal to the corresponding Z - $\alpha,\beta,\gamma,\delta$ -unsaturated amide ($1 \rightarrow 2$, eq 1) has been studied computationally at the CBS-QB3 level of theory. All competing mechanisms were also characterized with density functional theory (DFT) calculations, using B3LYP and M06-2X functionals with the triple- ζ 6-311+G(d,p) basis set. Full details of all the methods used and calculations performed are given in the Computational Methods at the end of the paper. In experiment, substrate **1** rearranges under microwave irradiation at 220 °C for 2 h, forming **2** with minor amounts of the E -diastereomer (9:1). At all levels examined, we find the mechanism shown in Scheme 2c to be preferred.



The results of our computational evaluation of the rearrangement mechanism in Scheme 2c are presented in Figure 1. To undergo pericyclic transformations by any of the mechanisms

under study, the substrate must first isomerize from the *trans*-configuration of one or both C=C bonds. Resonance effects present in the aminopentadienal will aid this process, by stabilizing the zwitterionic intermediate involving isomerization of the α,β -C=C bond to form **1**-(Z,E). Indeed, a dihedral scan showed that E to Z isomerization is strongly influenced by solvation, giving a computed B3LYP/6-311+G(d,p)//B3LYP/6-31G(d) barrier using geometries optimized in solvent of 28.4 kcal/mol (see the Supporting Information). This **1**-(Z,E) isomer is 2.7 kcal/mol above the starting E,E -diastereoisomer. From this point we find that an exocyclic, suprafacial, [1,5]-hydride shift of the formyl hydrogen to the 5-position proceeds via a transition structure (TS-3) 31.0 kcal/mol higher in free energy. Computation of the intrinsic reaction coordinate (IRC) confirmed that this transition state (TS) does indeed lead to a minimum on the potential energy surface, which is a ketene intermediate. The ketene thus formed from this transformation lies 9.7 kcal/mol above **1**-(E,Z), but ring-closing from addition of the amino group to the ketene is predicted to be facile in forming **6**, downhill by 4.8 kcal/mol. We were unable to locate TS-5 since formation of **6** is extremely facile: a constrained scan of the forming N...C distance (see the Supporting Information) showed the formation of **6** to be barrierless starting from the acyclic conformer of **4** with the amino group eclipsing the C=C bond. The Z - $\alpha,\beta,\gamma,\delta$ -unsaturated amide **2** is furnished by ring-opening of **6**, proceeding via TS-7, with a barrier of only 18.2 kcal/mol.

It has been shown with *ab initio* calculations by Birney⁹ and others¹⁰ that the transition states for cycloadditions, electrocyclizations, and sigmatropic rearrangements of α -oxoketenes are all essentially planar, in contrast to the distinctly nonplanar transition states calculated for hydrocarbon pericyclic reactions. The planarity of these transition structures prevents overlap of

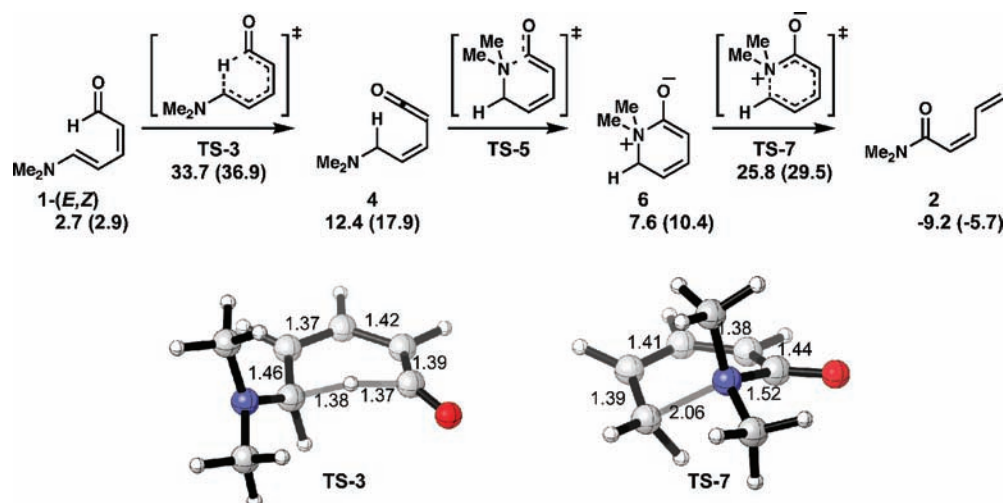


Figure 1. Favored mechanism for the rearrangement of Zincke aldehydes, corresponding to Scheme 2c. CBS-QB3 G_{rel} in kilocalories per mole. Values in parentheses incorporate a CPCM (conductor-like polarizable continuum model) solvation correction computed with B3LYP/6-311+G(d,p) to describe 1,2-dichlorobenzene.

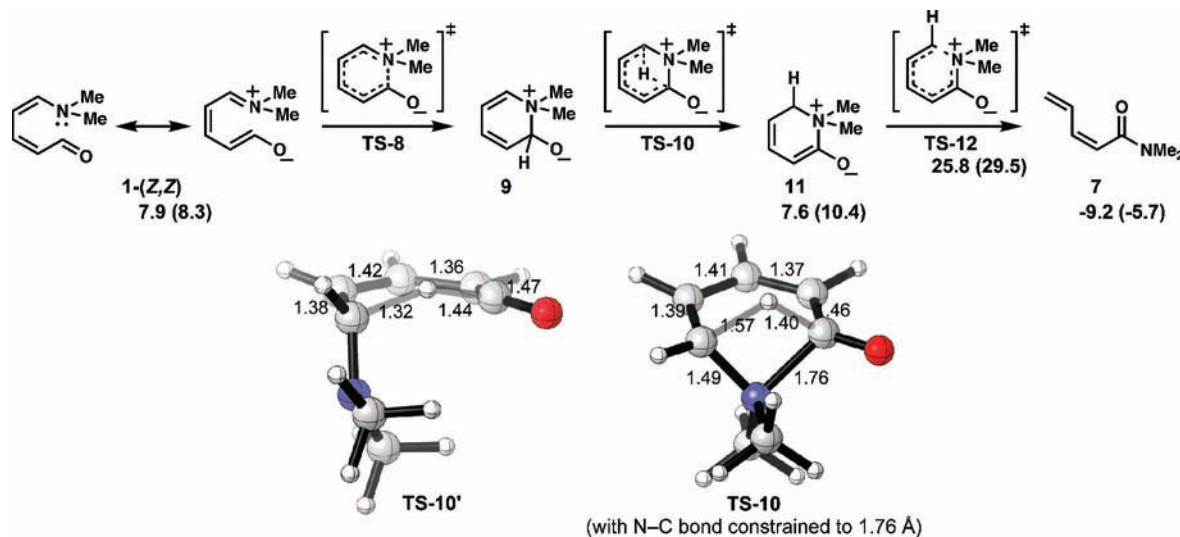


Figure 2. Previously proposed mechanism for Zincke aldehyde rearrangement, corresponding to Scheme 2b. CBS-QB3 G_{rel} in kilocalories per mole. Values in parentheses incorporate a CPCM solvation correction computed with B3LYP/6-311+G(d,p) to describe 1,2-dichlorobenzene.

the σ - and π -orbitals, in what Lemal has defined as a pseudopericyclic orbital topology.¹¹ The 6π -electrocyclic ring closure of azatrienes has been classified as either pseudopericyclic¹² or pericyclic¹³ on the basis of DFT calculations, or more recently as neither purely one nor the other extreme on the basis of CASSCF calculations.¹⁴ The defining characteristics of pseudopericyclic reactions as described by Birney are low or nonexistent barriers, planar transition structure geometries, and cyclic reactions that are allowed irrespective of the number of atoms.¹⁵ The nonplanarity of ring-opening TS-7 (Figure 1) is therefore more typical^{16,17} of a pericyclic than pseudopericyclic TS, but the orbital overlap is seemingly antarafacial, and the imaginary vibration reveals this TS to be conrotatory rather than disrotatory. The barrier for this ring-opening is also much lower than for the electrocyclic ring-opening of cyclohexadiene (47.7 kcal/mol at the CASPT2/6-31G(d) level¹⁴) and so could be interpreted as evidence for pseudopericyclic character. Indeed, calculation of the isotropic shielding tensor (using the gauge-invariant atomic

orbital method at the B3LYP/IGLO-III level of theory) at the center of cyclic TS-7 gives an NICS(0)_{iso} value of +0.5, which also suggests that this structure should not be considered as aromatic (nor pericyclic in a Dewar–Zimmerman sense) in contrast to a value of -13.5 for the pericyclic electrocyclic closing of cyclohexatriene. Alternatively, the ring-opening process could be assisted from the reservoir of electron density on the alkoxide oxygen.

Mechanistic possibility b (Scheme 2b), the one previously envisaged to be most likely, is considered next. Here, as shown in Figure 2, the substrate must isomerize both *trans* C=C bonds to form 1-(*Z,Z*), predicted to lie 7.9 kcal/mol above the *all-trans* substrate. Cyclization would ensue to form zwitterionic intermediate 9 via nucleophilic attack of the aldehyde by the amino group or 6π -electrocyclization. A [1,5]-hydride shift in this species was proposed to lead to the formation of 11, which could then undergo electrocyclic ring-opening to the rearranged product. However, attempts to locate postulated zwitterionic

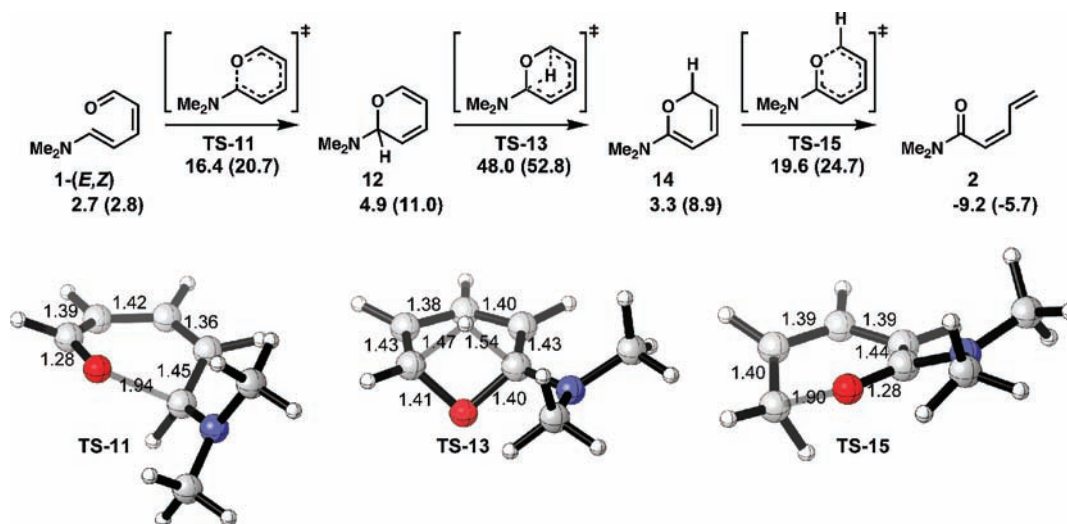


Figure 3. Alternative mechanism for Zincke aldehyde rearrangement, previously disproved experimentally. CBS-QB3 G_{rel} in kilocalories per mole. Values in parentheses incorporate a CPCM solvation correction computed with B3LYP/6-311+G(d,p) to describe 1,2-dichlorobenzene.

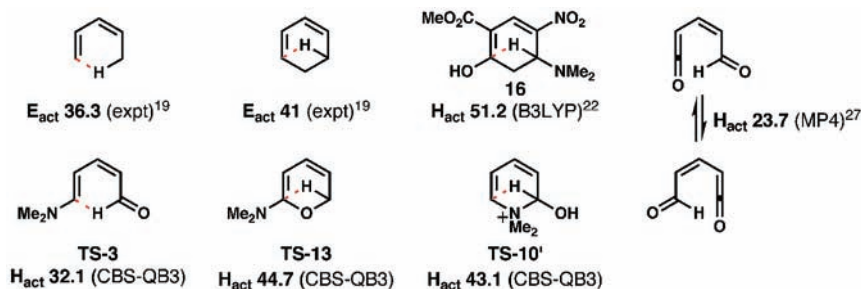


Figure 4. Comparison of [1,5]-hydride shifts in cyclic and acyclic systems. Energetics in kilocalories per mole.

intermediate **9** and transition structures TS-8 and TS-10 failed.¹⁸ Instead, optimization results in ring-opening. Attempts to optimize zwitterionic TS-10 resulted in an acyclic [1,5]-hydride shift TS, which was confirmed to lead to a ketene intermediate by IRC analysis (Figure 2, TS-10'). This TS is a configurational isomer of TS-3, less stable by 3.7 kcal/mol, but again points to a mechanism in which the hydride shift occurs before ring-closing.

Although we were unable to find them as stationary points on the potential energy surface, we sought to obtain an estimate for the energies of the elusive TS-8, intermediate **9**, and TS-10. After protonation of the aldehyde oxygen it was possible to optimize ring-closed intermediate **9-H**⁺ and the TS for the transannular [1,5]-hydride shift TS-10-H⁺ (not shown). The overall free energy barrier was found to be 47.4 kcal/mol, indicating that this process would be less favorable than the mechanism in Figure 1 by 13.7 kcal/mol and therefore uncompetitive. Alternatively, when we held the N–C bond constrained at 1.76 Å (equal to the value found in intermediate **6**) without protonation, a structure was optimized corresponding to TS-10 (Figure 2): this species lies 51.2 kcal/mol (M06-2X/6-311+G(d,p)) in free energy above **1**. This result again points to very high energy of transformations via this mechanism, particularly due to the previously envisaged transannular [1,5]-hydride shift.

We also considered mechanistic possibility a (Scheme 2a), in which cyclization occurs first to an intermediate pyran and is followed by a transannular [1,5]-hydride shift and electrocyclic ring-opening, with our computational results shown in Figure 3.

This mechanism has been discredited experimentally, because it incorrectly predicts the products of rearrangement of 2-substituted dienals. However, this was a useful test to ensure that our computations were in accord with what was known experimentally. The first step forming pyran **12** is predicted to be feasible; however, the transannular [1,5]-hydride shift TS-13 lies 48.0 kcal/mol above the starting material—much higher than that computed for the acyclic [1,5]-shift in our new proposed mechanism. Again, of interest are the computed B3LYP/IGLO-III NICS(0)_{iso} values for ring-closing TS-11 and ring-opening TS-15 of -1.4 and -3.6 ppm, respectively. These values are far from the characteristic range of -10 to -16 ppm that would be expected for an aromatic and, hence, pericyclic TS. That this mechanism is disfavored computationally as well as experimentally gave us confidence in the ability of the calculations to correctly rank the competing mechanisms.

The barrier for the rate-limiting [1,5]-hydride shift in the mechanism presented in Figure 1 is preferred by over 10 kcal/mol relative to the other pathways examined, providing strong support for this pathway. The favorability of a [1,5]-hydride shift in an acyclic precursor over a transannular process in cyclic substrates is also evident in the relative reactivities of 1,3-pentadiene and 1,3-cyclohexadiene: the activation barrier of the 1,5-hydride shift in 1,3-cyclohexadiene is over 5 kcal/mol larger than the corresponding shift in 1,3-pentadiene, as deduced experimentally¹⁹ and from DFT calculations²⁰ (41.9 vs 36.6 kcal/mol), due to the unfavorable formation of a four-membered ring

in the pericyclic transition structure of the transannular hydride shift (Figure 4).²¹ A related [1,5]-hydride shift was previously proposed to occur in polysubstituted aminocyclohexadiene **16** studied by Davies; however, computations from the Houk group showed that this barrier was much larger than those of competing pathways.²² The computed barrier for **TS-3** is lower than for the analogous [1,5]-hydride shift in 1,3-pentadiene; of relevance here are the observations of Okamura, who has reported that [1,5]-hydrogen migrations in systems where the terminal double bond of a polyene is replaced by an allene proceed with an activation energy 10–12 kcal/mol lower than for other typical [1,5]-migrations.²³ This effect has been studied computationally by Jensen,²⁴ who attributed the stabilizing effect of allenes on [1,3]- and [1,5]-hydride shifts to extra conjugation in the transition state. A similar rate-lowering effect has also been found in [1,5]-hydride shifts of ketenes.^{25,26} The [1,5]-hydride shift in ketene-containing 5-oxo-2,4-pentadienal has been characterized as pseudopericyclic, proceeding via a planar TS with an energetic barrier of just 23.7 kcal/mol.²⁷ The $\phi_{\text{CCC(N)H}}$ dihedral of **TS-3** of 28.1° is similar to that found in the [1,5]-hydride shift in 1,3-pentadiene (27.7°), suggesting that **TS-3** may be suitably described as pericyclic; however, the $\phi_{\text{CCC(O)H}}$ dihedral of **TS-3** is 7.0°, and such planarity may be used to infer a pseudopericyclic character. Natural bond orbital principal delocalizations obtained from second-order perturbation theory show the CH σ interaction with the CC π^* expected for a TS of pericyclic nature is worth 32.1 kcal/mol, while the CH σ interaction with the CO π^* of the developing ketene

(perpendicular to the ring) amounts to 52.0 kcal/mol.²⁸ These data, along with a computed B3LYP/IGLO-III NICS(0)_{iso} value of -6.5 ppm, suggests a mixing of pericyclic and pseudopericyclic orbital topologies, as Birney has suggested can occur when both are geometrically feasible and allowed.²⁹

In the reaction studied here, the preferred mechanism involves a transient ketene; we sought to trap this reactive functional group and to lend experimental credence for its intermediacy. Intermolecular trapping experiments were attempted by performing the rearrangement in alcoholic solvents, in the hope of obtaining ester products. These attempts were thwarted by the lack of rearrangement reactivity in these solvents. We next synthesized Zincke aldehyde **17** (Scheme 3), which bears a tethered hydroxyl group, which we hoped might result in lactone formation upon rearrangement. Of course, the dimethylamino group is much more nucleophilic than an alcohol; however, we expected that the equilibrium between ring-closed dihydropyridinium zwitterions **19** and aminoketene **18** would enable partitioning of the rearrangement products toward **21**. This expectation was not borne out by experiment: only cleanly rearranged diene product **20** was observed. This result in no way discounts the proposed mechanism (absence of evidence is not evidence of absence!), but only suggests that weaker nucleophiles cannot compete with the dimethylamino group.

With a new mechanism in hand, we sought to understand the effects of α - and β -substitution of the Zincke aldehyde on the rate of rearrangement (Table 1). Unsubstituted Zincke aldehyde **1**-(*E,E*) was combined with the 2-methyl substrate **22** in one flask and subjected to rearrangement conditions to ensure identical reaction conditions. A similar experiment was performed with **1**-(*E,E*) and 3-methyl Zincke aldehyde **23**. The relative rates of the rearrangement were determined by ¹H NMR. Transition states corresponding to **TS-3** and **TS-7** (see Figure 1) were calculated in each case, and the overall free energy barrier for the rearrangement process via our proposed mechanism was evaluated for each. Relative first-order rate constants were calculated from the conversion after 1 h under thermal conditions.

A good accord is achieved between experimental and computational results. Experiment reveals that 2-methylation retards the rearrangement, while 3-methylation accelerates it, and the computed barriers for rearrangement reflect this trend. The reaction of **1** is 5-fold faster than that of **22** at 200 °C, which equates to a $\Delta\Delta G^\ddagger$ of 1.6 kcal/mol, while the 8-fold faster

Scheme 3. Unsuccessful Attempt To Trap an Intermediate Ketene with a Tethered Hydroxyl Group

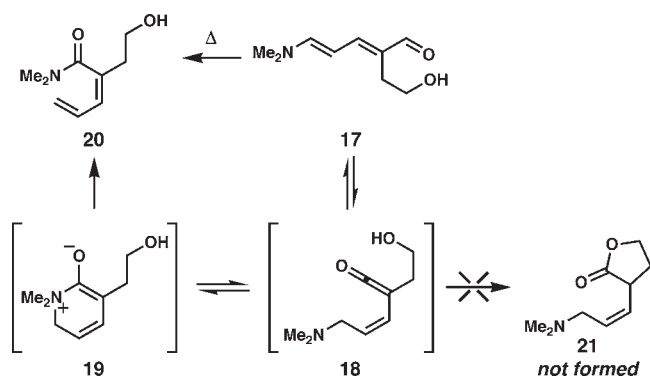


Table 1. Computed CBS-QB3 Free Energy Barriers/Changes (kcal/mol) Compared with Experimental Rates/Conversions^a

	G_1^\ddagger	$\Delta\Delta G^\ddagger$	G_2^\ddagger	ΔG_{rxn}	k_{rel}
1 , $R^1 = R^2 = \text{H}$	+33.7	0.0	+25.8	-9.2	1.0
22 , $R^1 = \text{Me}$, $R^2 = \text{H}$	+35.1	+1.4	+27.3	-7.8	0.2 ^b
23 , $R^1 = \text{H}$, $R^2 = \text{Me}$	+29.6	-4.1	+20.9	-12.1	>8.6 ^c

^a G_1^\ddagger and G_2^\ddagger refer to the free energies of 1,5-hydride shift and ring-opening TSs, respectively. $\Delta\Delta G^\ddagger$ refers to the difference in rate-limiting barrier heights with respect to substrate **1**. ^b At 200 °C, 1 h. ^c At 175 °C, 1 h.

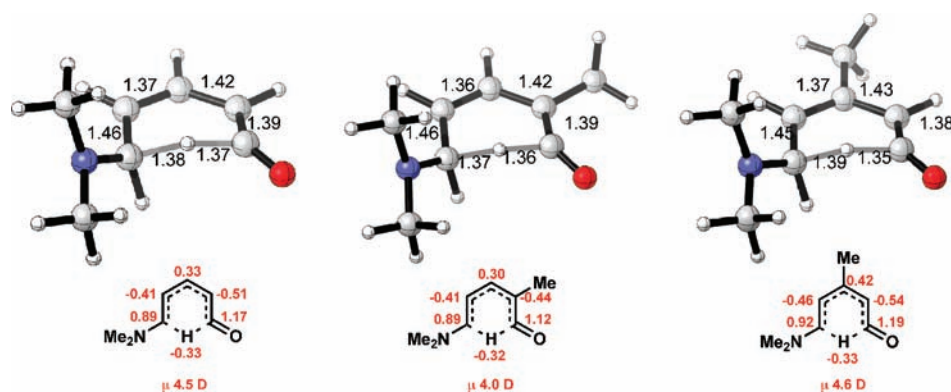


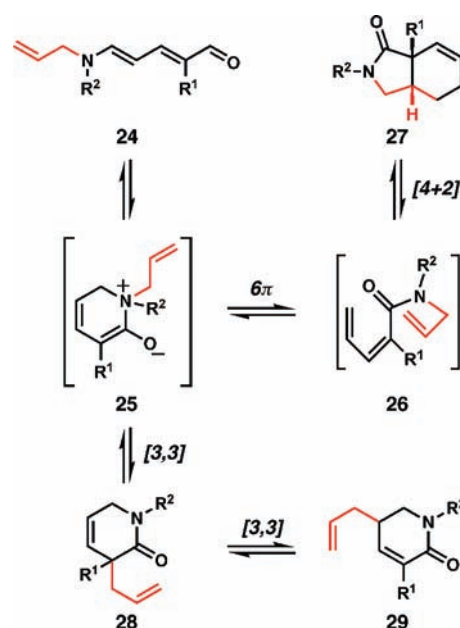
Figure 5. CBS-QB3-optimized [1,5]-hydride shift TSs with MP2/6-311+G(3d2f,2df,2p)-computed APT (atomic polar tensor) atomic charges (au) and dipole moments (D).

reaction of **23** relative to **1** at 175 °C equates to a $\Delta\Delta G^\ddagger$ of around 2.5 kcal/mol (for full derivation of these values, see the Supporting Information). CBS-QB3 barriers between **1** and **15** and **1** and **16** differ by 1.5 and 4.1 kcal/mol, respectively. The same trend in stability of the transition structures is also observed in the rearranged amide products. These differences in rate appear to be electronic in origin. The [1,5]-hydride shift TS is polarized with alternating positively and negatively charged carbons, consistent with a hydridic transfer (Figure 5); therefore, 2-methylation is at the site of negative charge, and destabilizes the transition state, while 3-methylation stabilizes positive charge at that position. In addition to TS stabilization, methylation may also destabilize to different extents the planar *E,E*-reactant geometry and rate-limiting TS through unfavorable steric interactions, thus contributing to observed rate differences.

Zincke aldehydes derived from allylic amines (**24**, Scheme 4) undergo a cascade of further rearrangements to give bicyclic lactams **27** and dihydropyridones **28/29**.⁴ An intramolecular Diels–Alder cycloaddition can follow the electrocyclic ring-opening in the Zincke aldehyde rearrangement pathway to provide bicyclic lactam **27**. Alternatively, instead of ring-opening via electrocyclic ring-opening, a [3,3]-sigmatropic rearrangement with charge neutralization can occur to form dihydropyridone **28**, which itself may rearrange further by a terminal Cope rearrangement to **29**. Computations were used to assess the mechanisms of these finely balanced pathways and to identify at which stage the product selectivity is determined.

Upon heating, diallylamine-derived Zincke aldehyde (here one of the allyl groups in the substrate is modeled in our computations by a smaller methyl group, i.e., substrate **30a**) gave predominantly Diels–Alder adduct **35a** (48%, >10:1 dr) with a lesser amount (3%) of the product from sigmatropic rearrangement (**37**). The results of calculations into the competing mechanisms are shown in Figure 6. For the pathway leading to the formation of bicyclic lactam **35a** from common zwitterionic intermediate **31a**, the rate-limiting step is clearly electrocyclic ring-opening: the intramolecular Diels–Alder (IMDA) reaction via **TS-34a** is predicted to be relatively facile by comparison and largely irreversible due to the large exergonicity of the process. In the competing pathway leading to dihydropyridones **37a** and **39a**, the first [3,3]-rearrangement is computed to be rate-limiting and largely irreversible since the formation of dihydropyridone **37a** is downhill by 33.9 kcal/mol; charge neutralization might be expected to play a major role. However,

Scheme 4. Bicyclic Lactams and/or Dihydropyridones Result from the Rearrangement of Allylic Amine-Derived Zincke Aldehydes



the subsequent Cope rearrangement via **TS-38a** interconverting the isomeric dihydropyridones has a TS much lower in free energy than that for the initial sigmatropic rearrangement, so one should expect that the ratio of **37a** to **39a** is largely controlled by thermodynamic stability rather than kinetics. Our calculations show that the ratio of bicyclic lactam to dihydropyridone is controlled by the ease of electrocyclic ring-opening vs the first [3,3]-sigmatropic rearrangement, that is, the relative free energies of **TS-32a** and **TS-36a**. The experimentally observed preference for the bicyclic lactam is reproduced by all levels of theory tested (B3LYP, M06-2X, and CBS-QB3). The quantitative agreement between theory and experiment is good: the experimental 16:1 ratio of **35a** to **37a** at 200 °C equates to a $\Delta\Delta G^\ddagger$ of 2.6 kcal/mol for **TS-32a** and **TS-36a**, compared with the computed M06-2X free energy difference of 3.0 kcal/mol. Interconversion between dihydropyridones **37a** and **39a** is expected to be facile, since **TS-38** is relatively low in energy, so that the ratio of these sigmatropic

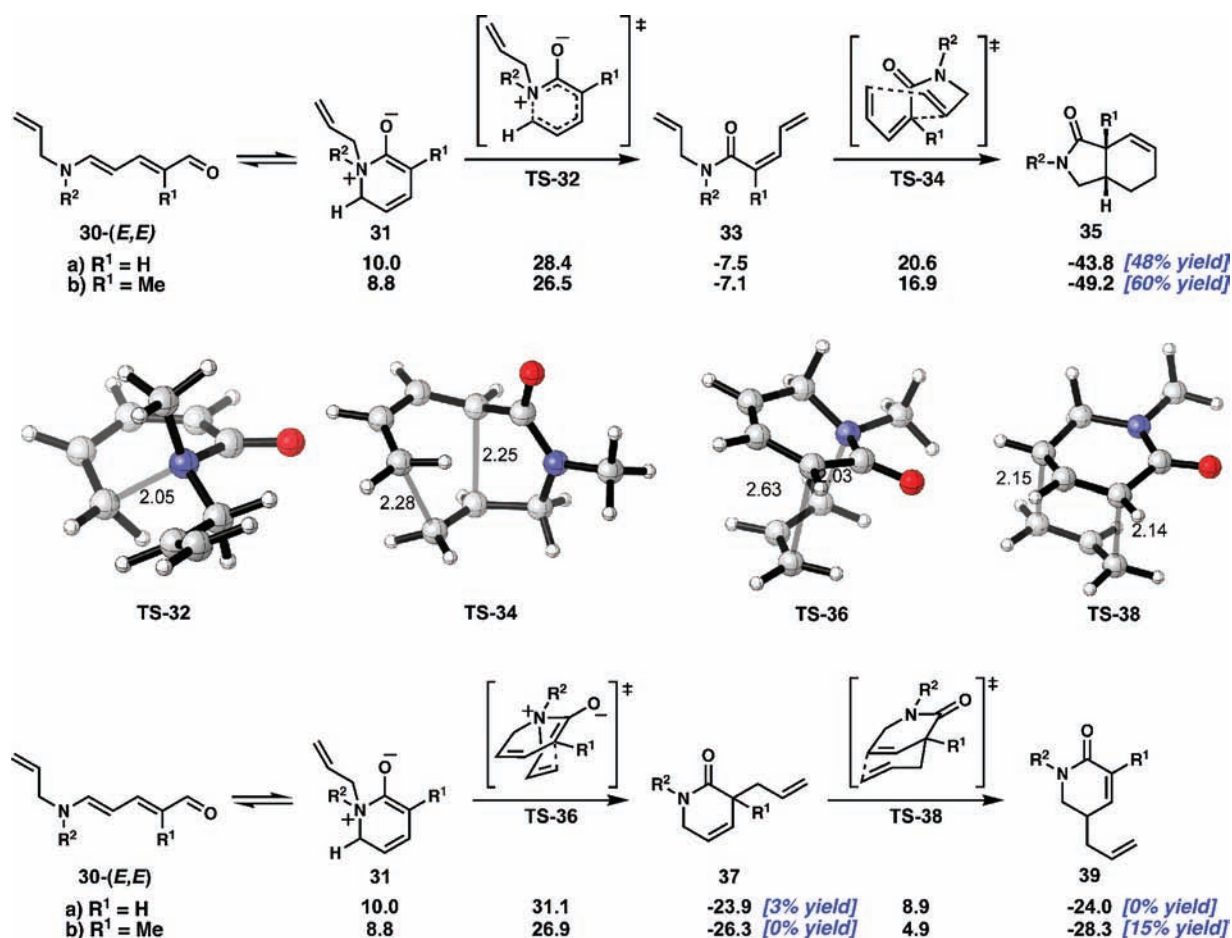


Figure 6. Competing pericyclic pathways for *N*-allyl Zincke aldehydes, with M06-2X/6-311+G(d,p)//B3LYP/6-311+G(d,p) G_{rel} in kilocalories per mole. Calculations performed for R² = methyl, experiments performed for R² = allyl.

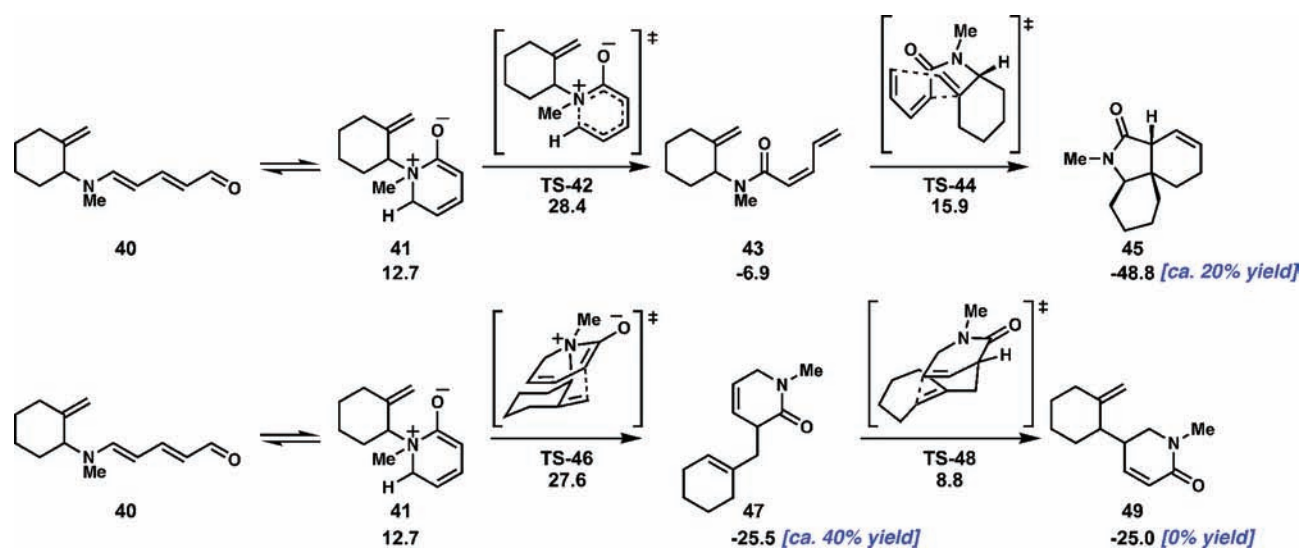


Figure 7. Competing pericyclic pathways for *N*-allyl Zincke aldehyde 40, with M06-2X/6-311+G(d,p)//B3LYP/6-311+G(d,p) G_{rel} in kilocalories per mole.

isomers should reflect their thermodynamic stabilities. In experiment, the α -unsubstituted Zincke aldehyde 30a forms only dihydropyridone 37a, while the α -methyl Zincke aldehyde

substrate 30b gives only the further rearranged isomer 39b. The computed free energy difference is small for dihydropyridones 37a and 39a, but the computed difference in the case with

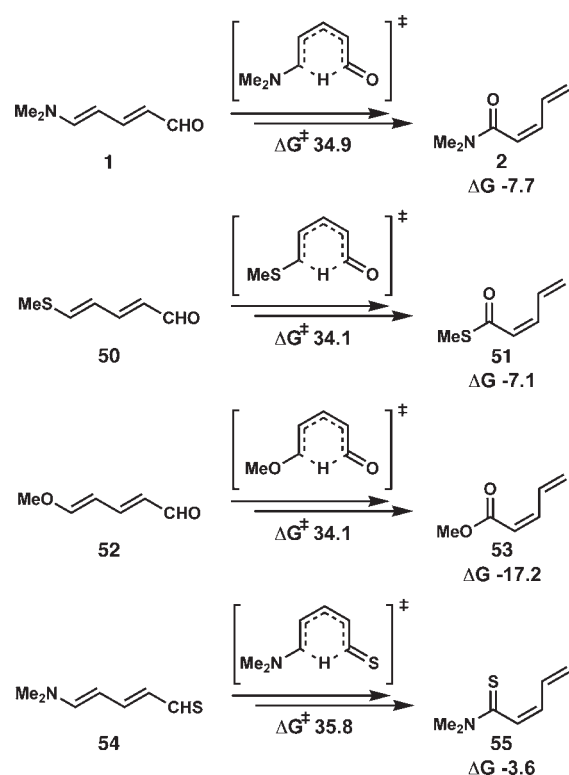


Figure 8. Computed barriers and free energy changes for Zincke aldehyde structural analogues undergoing the same thermal rearrangement, with M062X/6-311+G(d,p)/B3LYP/6-311+G(d,p) G_{rel} in kilocalories per mole.

α -methyl substitution increases to 2.0 kcal/mol in favor of the conjugated lactam corresponding to **39b**. In the rearrangement of **30b**, good qualitative agreement is observed between calculation and experiment: the much lower ratio (ca. 4:1) of Diels–Alder product to dihydropyridone product compared to that observed with unsubstituted substrate **30a** is accompanied by a calculated difference in **TS-32b** and **TS-36b** of only 0.4 kcal/mol. Similarly, the exclusive formation of conjugated dihydropyridone **39b** at the expense of less stable **37b** is perfectly consistent with the computational results.

The one outlier that preferentially produces the [3,3]-rearrangement product is substrate **40** (Figure 7), whose allylamino function is constrained to a ring; with this substrate, the IMDA adduct is the minor component of a 2:1 mixture of products. This experimental result indicates that the [3,3]-rearrangement should be favored over the electrocyclic ring-opening for the zwitterionic intermediate derived from this substrate. Computations on this system show that the balance between **TS-42** and **TS-46** now lies in favor of the [3,3]-sigmatropic pathway, which is preferred by 0.8 kcal/mol. The computed selectivity is therefore in qualitative and also quantitative agreement with experiment, since the experimental 2:1 selectivity corresponds to a free energy difference between the competing electrocyclic and sigmatropic TSs of 0.6 kcal/mol.

Because of the clear utility of the Zincke aldehyde rearrangement reactions, we studied computationally the rearrangements of related donor–acceptor dienes to predict their thermodynamic and kinetic feasibility. 5-(Alkylthio)-2,4-dienals and 5-alkoxy-2,4-dienals (**50** and **52**, Figure 8) should rearrange to **51** and **53**, respectively, with activation barriers for the rate-limiting

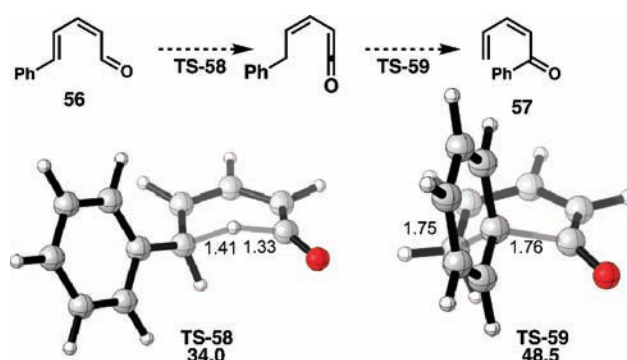


Figure 9. [1,5]-hydrogen transfer and [1,5]-phenyl transfer in a 5-phenyl-2,4-dienal analogue, with M062X/6-311+G(d,p)/B3LYP/6-311+G(d,p) G_{rel} in kilocalories per mole.

[1,5]-H shift that are nearly identical to that of the corresponding Zincke aldehyde. The ester-forming reaction appears to be highly thermodynamically favored. Finally, doubly vinylous thioamide **54** has a slightly higher barrier for the sigmatropic shift and is the least exergonic of any of the variants. Unfortunately, all efforts to corroborate these computational results experimentally have so far not been fruitful. Although small samples of the sulfur and oxygen analogues **50** and **52** of the Zincke aldehyde could be made painstakingly, the rearrangement reactions of these substrates were unsuccessful. While starting materials were completely consumed upon heating, no identifiable products could be isolated and characterized. We hypothesize that the temperatures required to effect the pericyclic cascade led to polymerization of the presumably very reactive conjugated acrylate and thioacrylate esters. Although thioamides and vinylous thioamides are readily made by treatment of the corresponding carbonyl compounds with typical thionating reagents (Lawesson's reagent, for example),³⁰ in no cases could we isolate thiocarbonyl substrate **54**; therefore, we were never able to evaluate this rearrangement reaction.

In addition to the rearrangement of substrates containing N, O, and S heteroatoms in the 5-position to the corresponding amide, ester, and thioester, we have also investigated the potential of these rearrangements to form a phenyl ketone from the rearrangement of a 5-phenyl-2,4-dienal (**56** \rightarrow **57**, Figure 9). The barrier for [1,5]-hydride shift via **TS-58** is approximately the same as that for the unsubstituted Zincke aldehyde (34.0 kcal/mol), indicating that this step should occur. However, unlike the Zincke aldehyde substrate, ring-closing is unfavorable. The ring-closing and subsequent electrocyclic ring-opening steps that accomplish the migration of nitrogen in the Zincke aldehyde rearrangement are less favorable when migrating the phenyl group, but we envisaged that this migration could possibly occur directly via [1,5]-shift, as seen in **TS-59**. This transformation lies 48.5 kcal/mol above the starting material, so the overall transformation would be unexpected to occur on the basis of these computations.

The only closely related rearrangement that we have found in the literature involves rearrangement of 5-(methylthio)-2,3,4,5-tetrachloro-2,4-dienal **60** (Figure 10) and related compounds to the corresponding Z-thioesters, such as **66**, reported by Roedig and Goepfert.³⁰ This transformation proceeds under remarkably milder conditions (in carbon tetrachloride at reflux) than the rearrangement of Zincke aldehydes. We characterized computationally the three conceivable mechanisms in the same way as we

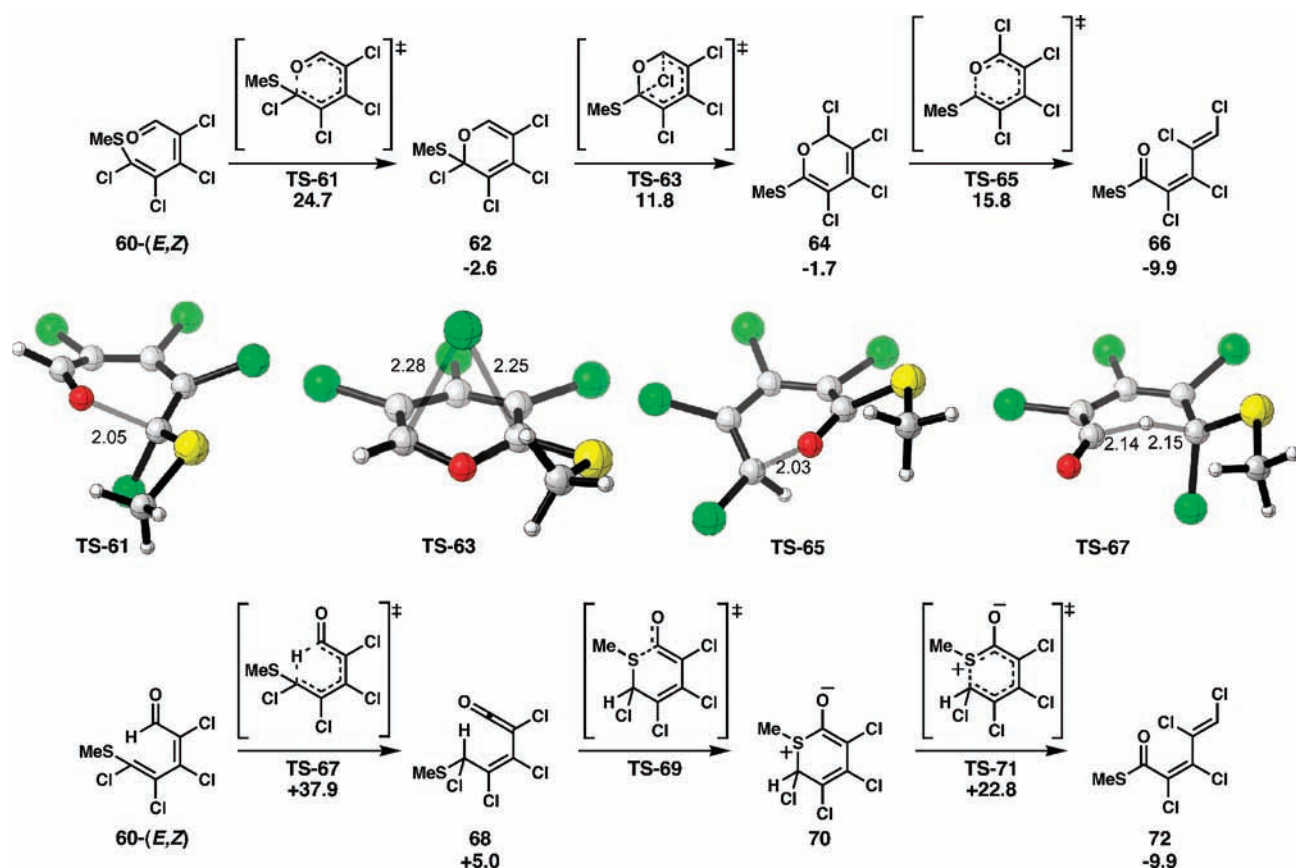


Figure 10. Mechanisms for the rearrangement of 5-(methylthio)-2,3,4,5-tetrachloro-2,4-dienal, with M062X/6-311+G(d,p)//B3LYP/6-311+G(d,p) G_{rel} in kilocalories per mole.

had for the Zincke aldehydes in Figures 1–3 to investigate if a similar mechanism is applicable here and to rationalize the greater reactivity of substrate **60**. The results of these calculations are shown in the figure.

In stark contrast to the Zincke aldehyde rearrangement, for which the pathway involving a pyran intermediate was ruled out experimentally and computationally, here we find that this mechanistic pathway is most favorable. Electrocyclization via **TS-61** to form a pyran intermediate has a barrier of 24.7 kcal/mol, which is rate limiting. The subsequent [1,5]-shift involves chloride, not hydride, and possesses a significantly lower barrier via **TS-63** than any of the [1,5]-hydride shifts calculated in this work. Electrocyclic ring-opening then occurs with a similarly low barrier to form *Z*-thioester product **66**. The rate-limiting TS lies only 24.7 kcal/mol above the starting substrate, which compares with the value of 33.7 kcal/mol obtained for the Zincke aldehydes by our newly proposed mechanism and 48.0 kcal/mol for the Zincke aldehyde mechanism involving a pyran intermediate. Therefore, we predict that polychlorinated dienals react via a different mechanism to the Zincke aldehydes with a barrier lower by 9.0 kcal/mol, which is consistent with the much milder conditions required for their rearrangement. The barriers and intermediates for substrate **60** undergoing rearrangement by the mechanism favored by Zincke aldehydes are similar to those calculated for the aminodienal, but the [1,5]-hydride shift via **TS-67** is much more difficult than the [1,5]-chloride shift, clearly indicating that the pyran-based mechanism is more likely for these substrates. The last

mechanistic possibility that we evaluated, corresponding to Zincke aldehyde rearrangement mechanism b (Scheme 2b), suffers from the same problems as for the aminodienal, since the substrate is unable to form a cyclized zwitterionic intermediate (calculations not shown).

CONCLUSIONS

Computational study of the thermal pericyclic cascade reactions of Zincke aldehydes has yielded important mechanistic insight into these rearrangements. We have discounted the previously postulated mechanism involving the sequence of ring closure, transannular [1,5]-sigmatropic shift of hydrogen, and electrocyclic ring-opening in favor of an order of events that begins with the sigmatropic shift in an acyclic intermediate to generate a vinylketene intermediate. Although experimental attempts to trap the presumed ketene intermediate were not successful, the experimentally observed rate dependence on alkyl substitution was well supported by computational results. Furthermore, the balance between diverging pericyclic processes in the thermal rearrangement reactions of Zincke aldehydes derived from allylic amines also demonstrates an excellent match between calculation and experimental results. Finally, computations suggest that similar rearrangements of a series of different donor–acceptor dienes should also be feasible, and we rationalize the lower temperature requirement of a previously known rearrangement of a related tetrachlorinated donor–acceptor diene by virtue of a change in mechanism. The data provided

here should facilitate the development of further useful pericyclic cascade reactions.

COMPUTATIONAL METHODS

All stationary points were fully optimized with Gaussian 09³¹ using the CBS-QB3 composite ab initio method, unless otherwise stated.³³ The complete basis set (CBS) methods remove error in quantum mechanical calculations that arise from the truncation of basis sets. The CBS models extrapolate to an infinite basis set limit by using an N^{-1} asymptotic convergence of MP2 pair energies calculated from pair natural orbital expansions. The CBS-QB3 method has a maximum error of 2.8 kcal/mol for the G2 test set and average and mean absolute errors of 0.20 and 0.98 kcal/mol. On a B3LYP/6-311G(d,p) geometry, energy corrections computed at the MP2, MP4(SDQ), and CCSD(T) levels of theory are used to give a final CBS-QB3 energy. Of particular relevance to this study, the CBS-QB3 method computes activation energies for a set of hydrocarbon pericyclic reactions to give a mean absolute error of 2.3 kcal/mol.³⁴ We also performed optimizations with the less demanding B3LYP hybrid density functional in combination with the 6-311+G(d,p) basis set.³⁵ A fine grid density was used for numerical integration in all DFT calculations. Harmonic vibrational frequencies were computed for all optimized structures to verify that they were either minima or transition states, possessing zero imaginary frequencies and one imaginary frequency, respectively. This level of DFT calculation has been shown to compute relative transition-state energies to compute selectivities that give good quantitative agreement with experiment.³⁶ Single-point energy calculations were also performed with the more recently parametrized M06-2X functional,³⁷ which is constructed to include nonlocal effects of electronic dispersion and is found to give good estimates for reaction enthalpies in bond-forming reactions. All levels examined led to the same conclusions, and in particular, the agreement between M06-2X and the CBS-QB3 results for the barriers and energy changes shown in Figures 1–3 was quantitatively very close. Therefore, in our studies on the larger systems which precluded the use of the demanding CBS-QB3 calculations, we relied on the computed M06-2X energetics to evaluate the competing mechanisms. A full comparison of all computed energetics at the different levels of theory is reported in full in the Supporting Information. Natural bond orbital (NBO) calculations were performed using NBO version 3.1 in Gaussian 09,³⁸ and principal delocalizations were quantified from second order perturbation theory analysis of the Fock matrix on the basis of the NBOs.

ASSOCIATED CONTENT

S Supporting Information. Characterization data and experimental procedures for all new compounds, B3LYP/6-311+G(d,p) and M06-2X/6-311+G(d,p) absolute energies, CBS-QB3 zero-point inclusive absolute enthalpies, free energies, and optimized Cartesian coordinates of all stationary points and imaginary vibrational frequencies where appropriate, and complete ref 32. This material is available free of charge via the Internet at <http://pubs.acs.org>.

AUTHOR INFORMATION

Corresponding Author

cdv@uci.edu; houk@chem.ucla.edu

ACKNOWLEDGMENT

We are grateful to the Royal Commission for the Exhibition of 1851 for a Research Fellowship (R.S.P.) and the California Tobacco-Related Disease Research Program and Eastman Chemicals

for graduate fellowships (S.E.S.). C.D.V. acknowledges support from the National Science Foundation (CAREER Award CHE-0847061), an Amgen Young Investigator Award, and an Astra-Zeneca Award for Excellence in Chemistry. C.D.V. is a fellow of the A. P. Sloan Foundation. Computations were performed using the UCLA Academic Technology Services Hoffman2 Beowulf cluster and the San Diego Supercomputer Center Thresher cluster.

REFERENCES

- (1) Steinhardt, S. E.; Silverston, J. S.; Vanderwal, C. D. *J. Am. Chem. Soc.* **2008**, *130*, 7560–7561.
- (2) (a) Zincke, T. *Liebigs Ann. Chem.* **1903**, *330*, 361–374. (b) Zincke, T. *Liebigs Ann. Chem.* **1904**, *333*, 296–345. (c) Zincke, T.; Wurker, W. *Liebigs Ann. Chem.* **1905**, *338*, 107–141. (d) König, W. *J. Prakt. Chem.* **1904**, *69*, 105–137.
- (3) For reviews, see: (a) Becher, J. *Synthesis* **1980**, 589–612. (b) Becher, J.; Finsen, L.; Winckelmann, I. *Tetrahedron* **1981**, *37*, 2375–2378. (c) Cheng, W.-C.; Kurth, M. J. *Org. Prep. Proced. Int.* **2002**, *34*, 587–608.
- (4) Steinhardt, S. E.; Vanderwal, C. D. *J. Am. Chem. Soc.* **2009**, *131*, 7546–7547.
- (5) Kearney, A. M.; Vanderwal, C. D. *Angew. Chem., Int. Ed.* **2006**, *45*, 7803–7806.
- (6) Michels, T. D.; Rhee, J. U.; Vanderwal, C. D. *Org. Lett.* **2008**, *10*, 4787–4790.
- (7) (a) Martin, D. B. C.; Vanderwal, C. D. *J. Am. Chem. Soc.* **2009**, *131*, 3472–3473. (b) Martin, D. O. C.; Vanderwal, C. D. *Chem. Sci.* Published online on 4 February 2011; DOI: 10.1039/C1SC00009H.
- (8) Michels, T. D.; Kier, M. J.; Kearney, A. M.; Vanderwal, C. D. *Org. Lett.* **2010**, *12*, 3093–3095.
- (9) (a) Ham, S.; Birney, D. M. *Tetrahedron Lett.* **1994**, *35*, 8113–8116. (b) Birney, D. M.; Wagenseller, P. E. *J. Am. Chem. Soc.* **1994**, *116*, 6262–6270. (c) Birney, D. M. *J. Org. Chem.* **1994**, *59*, 2557–2564. (d) Wagenseller, P. E.; Birney, D. M.; Roy, D. *J. Org. Chem.* **1995**, *60*, 2853–2859.
- (10) (a) Nguyen, M. T.; Ha, T.; More O'Ferrall, R. A. *J. Org. Chem.* **1990**, *55*, 3251–3256. (b) Allen, A. D.; McAllister, M. A.; Tidwell, T. T. *Tetrahedron Lett.* **1993**, *34*, 1095–1098. (c) Wong, M. W.; Wentrup, C. *J. Org. Chem.* **1994**, *59*, 5279–5285. (d) Hong, S. G.; Fu, X. Y. *J. Mol. Struct.: THEOCHEM* **1990**, *209*, 241.
- (11) Ross, J. A.; Seiders, R. P.; Lemal, D. M. *J. Am. Chem. Soc.* **1976**, *98*, 4325–4327.
- (12) (a) de Lera, A. R.; Alvarez, R.; Lecea, B.; Torrado, A.; Cossio, F. P. *Angew. Chem., Int. Ed.* **2001**, *40*, 557–561. (b) de Lera, A. R.; Cossio, F. P. *Angew. Chem., Int. Ed. Engl.* **1995**, *117*, 12314–12321.
- (13) Rodríguez-Otero, J.; Cabaleiro-Lago, E. *Angew. Chem., Int. Ed.* **2002**, *41*, 1147–1150.
- (14) Duncan, J. A.; Calkins, D. E. G.; Chavarha, M. *J. Am. Chem. Soc.* **2008**, *130*, 6740–6748.
- (15) Zhou, C.; Birney, D. M. *J. Am. Chem. Soc.* **2002**, *124*, 5231–5241.
- (16) Houk, K. H.; Gonzalez, J.; Li, Y. *Acc. Chem. Res.* **1995**, *28*, 81–90.
- (17) Birney, D. M.; Xu, X.; Ham, S. *Angew. Chem., Int. Ed.* **1999**, *38*, 189–193.
- (18) These species were not minima on the potential energy surface computed with the B3LYP, MP2, and M06-2X level and with MPWIK, recently recommended for optimizing zwitterions: Wei, Y.; Sateesh, B.; Maryasin, B.; Sastry, G. N.; Zipse, H. *J. Comput. Chem.* **2009**, *30*, 2617–2624.
- (19) The observed activation energy for the 1,5-hydride shift in 1,3-pentadiene is 36.3 kcal/mol: Roth, W. R.; König, J. *Justus Liebigs Ann. Chem.* **1966**, 699. The value for 1,3-cyclohexadiene is 41 kcal/mol: de Dobbelaere, J. R.; van Zeeventer, E. L.; de Haan, J. W.; Buck, H. M. *Theor. Chim. Acta* **1975**, *38*, 241.
- (20) (a) Jensen, F.; Houk, K. N. *J. Am. Chem. Soc.* **1987**, *109*, 3139–3140. (b) Houk, K. N.; Li, Y.; Evanseck, J. D. *Angew. Chem., Int. Ed. Engl.*

1992, 31, 682–708. (c) Hess, B. A., Jr.; Baldwin, J. E. *J. Org. Chem.* **2002**, 67, 6025–6033. (d) Alabugin, I. V.; Manoharan, M.; Breiner, B.; Lewis, F. D. *J. Am. Chem. Soc.* **2003**, 125, 9329–9342. (e) Guner, V.; Khuong, K. S.; Leach, A. G.; Lee, P. S.; Bartberger, M. D.; Houk, K. N. *J. Phys. Chem. A* **2003**, 107, 11445–11459.

(21) Tantillo, D. J.; Hoffmann, R. *Eur. J. Org. Chem.* **2004**, 273–280.

(22) (a) Davies, I. W.; Marcoux, J.-F.; Kuethe, J. T.; Lankshear, M. D.; Taylor, J. D. O.; Tsou, N.; Dormer, P. G.; Hughes, D. L.; Houk, K. N.; Guner, V. *J. Org. Chem.* **2004**, 69, 1298–1308. (b) Guner, V. A.; Houk, K. N.; Davies, I. W. *J. Org. Chem.* **2004**, 69, 8024–8028.

(23) (a) Shen, G.-Y. T.; Tapai, K.; Okamura, W. H. *J. Am. Chem. Soc.* **1987**, 109, 7499. (b) Barrack, S. A.; Okamura, W. H. *J. Org. Chem.* **1986**, 51, 3201. (c) Elnagar, H. Y.; Okamura, W. H. *J. Org. Chem.* **1988**, 53, 3060. (d) Palenzuale, J. A.; Elnagar, H. Y.; Okamura, W. H. *J. Am. Chem. Soc.* **1989**, 111, 1770. (e) Okamura, W. H. *Acc. Chem. Res.* **1983**, 16, 81. (f) Curtin, M. L.; Okamura, W. H. *J. Am. Chem. Soc.* **1991**, 113, 6958. (g) Okamura, W. H.; Elnagar, H. Y.; Ruther, M.; Dobreff, S. *J. Org. Chem.* **1993**, 58, 600.

(24) Jensen, F. *J. Am. Chem. Soc.* **1995**, 117, 7487–7492.

(25) Ramana Rao, V. V.; Fulloon, B. E.; Bernhardt, P. V.; Koch, R.; Wentrup, C. *J. Org. Chem.* **1998**, 63, 5779–5786.

(26) Sigalov, M.; Rappoport, Z. *J. Chem. Soc., Perkin Trans. 2* **1997**, 1911–1912.

(27) Birney, D. M. *J. Org. Chem.* **1996**, 61, 243–251.

(28) Alajarin, M.; Ortín, M.; Sánchez-Andrada, P.; Vidal, A. *J. Org. Chem.* **2006**, 71, 8126–8139.

(29) Ji, H.; Li, L.; Xu, X.; Ham, S.; Hammad, L. A.; Birney, D. M. *J. Am. Chem. Soc.* **2009**, 131, 528–537.

(30) For example, see: Shabana, R.; Rasmussen, J. B.; Olesen, S. O.; Lawesson, S.-O. *Tetrahedron* **1980**, 36, 3047–3051.

(31) Roedig, A.; Goepfert, H. *Chem. Ber.* **1981**, 114, 3625–3633.

(32) Frisch, M. J.; et al. *Gaussian 09*, revision A.02; Gaussian, Inc.: Wallingford, CT, 2009.

(33) (a) Montgomery, J. A., Jr.; Frisch, M. J.; Ochterski, J. W.; Petersson, G. A. *J. Chem. Phys.* **1999**, 110, 2822–2827. (b) Montgomery, J. A., Jr.; Frisch, M. J.; Ochterski, J. W.; Petersson, G. A. *J. Chem. Phys.* **2000**, 112, 6532–6542.

(34) Ess, D. H.; Houk, K. N. *J. Phys. Chem. A* **2005**, 109, 9542–9553.

(35) (a) Becke, A. D. *J. Chem. Phys.* **1993**, 98, 5648–5652. (b) Lee, C.; Yang, W.; Parr, R. G. *Phys. Rev. B* **1988**, 37, 785–789. (c) Vosko, S. H.; Wilk, L.; Nusair, M. *Can. J. Phys.* **1980**, 58, 1200–1211. (d) Stephens, P. J.; Devlin, F. J.; Chabalowski, C. F.; Frisch, M. J. *J. Phys. Chem.* **1994**, 98, 11623–11627.

(36) (a) Hayden, A. E.; Paton, R. S.; Becker, J.; Lim, Y. H.; Nicolaou, K. C.; Houk, K. N. *J. Org. Chem.* **2010**, 75, 922–928. (b) Cheong, P. H.-Y.; Paton, R. S.; Bronner, S. M.; Im, G.-Y. J.; Garg, N. K.; Houk, K. N. *J. Am. Chem. Soc.* **2010**, 132, 1267–1269. (c) Paton, R. S.; Mackey, J. L.; Kim, W. H.; Lee, J. H.; Danishefsky, S. J.; Houk, K. N. *J. Am. Chem. Soc.* **2010**, 132, 9335–9340.

(37) Zhao, Y.; Truhlar, D. G. *Theor. Chem. Acc.* **2008**, 120, 215–241.

(38) Glendening, E. D.; Reed, A. E.; Carpenter, J. E.; Weinhold, F. NBO Version 3.1.